

To appear in *Mathematical and Computer Modelling of Dynamical Systems*
Vol. 00, No. 00, Month 20XX, 1–14

ORIGINAL ARTICLE

Galerkin approximations with embedded boundary conditions for retarded delay differential equations

Z. Ahsan^a, T. Uchida^b, and C. P. Vyasarayani^{a*}

^a*Department of Mechanical and Aerospace Engineering, Indian Institute of Technology Hyderabad, Ordnance Factory Estate, Yeddumailaram 502205, Andhra Pradesh, India;*

^b*Department of Bioengineering, Stanford University, 318 Campus Drive, James H. Clark Center, Stanford, CA 94305-5448, U.S.A.*

(April 12, 2015)

Finite-dimensional approximations are developed for retarded delay differential equations (DDEs). The DDE system is equivalently posed as an initial–boundary value problem consisting of hyperbolic partial differential equations (PDEs). By exploiting the equivalence of partial derivatives in space and time, we develop a new PDE representation for the DDEs that is devoid of boundary conditions. The resulting boundary condition–free PDEs are discretized using the Galerkin method with Legendre polynomials as the basis functions, whereupon we obtain a system of ordinary differential equations (ODEs) that is a finite-dimensional approximation of the original DDE system. We present several numerical examples comparing the solution obtained using the approximate ODEs to the direct numerical simulation of the original nonlinear DDEs. Stability charts developed using our method are compared to existing results for linear DDEs. The presented results clearly demonstrate that the equivalent boundary condition–free PDE formulation accurately captures the dynamic behaviour of the original DDE system, and facilitates the application of control theory developed for systems governed by ODEs.

Keywords: boundary condition; delay differential equation; Galerkin method; retarded DDE; stability

AMS Subject Classification: 34D20, 35L04, 70E50, 70E55

1. Introduction

Mathematical models involving delay differential equations (DDEs) [1] are used to represent time-delay effects in a wide range of engineering systems. Examples include control systems [2], biological processes [3], machine tool vibration [4, 5], fluid–structure interaction [6], and traffic flow modelling [7]. DDEs are infinite-dimensional systems since we must specify an initial function [1] to obtain a unique solution.

The infinite-dimensional nature of DDEs complicates their analysis. We can always pose a DDE as an equivalent hyperbolic partial differential equation (PDE) constrained by a nonlinear boundary condition [8–10]. The mathematical representation of the PDE system appears to be more complicated than that of the original DDE; however, several methods are available for converting the PDE into a system

*Corresponding author. Email: vcprakash@iith.ac.in

of simple ordinary differential equations (ODEs) [11]. We, thus, arrive at a finite-dimensional ODE approximation of the original DDE, and can then make use of existing algorithms for the integration and continuation of these ODEs [12, 13]. Therein lies the benefit of this approach: by converting DDEs into systems of ODEs, we can exploit all existing tools developed for ODE systems to analyze the original DDEs.

Galerkin methods [11] are considered to be the optimal choice for obtaining reduced-order models for PDEs; however, in the case of a DDE-equivalent PDE, one must also handle the nonlinear boundary condition. Once a PDE has been discretized, the boundary condition can be incorporated using a Lagrange multiplier [14] or by employing the tau method [8, 15, 16]. In this work, we propose a formulation in which the boundary condition is completely eliminated and embedded directly into the PDE. Consequently, no special treatment of the boundary condition is necessary when applying the Galerkin method.

The paper is organized as follows. In Section 2, we present the class of DDEs in which we are interested, formulate the equivalent PDEs, eliminate the boundary conditions, and develop Galerkin approximations using Legendre polynomials as the basis functions. This particular choice of basis functions allows us to obtain explicit expressions for the finite-dimensional ODEs. In Section 3, we validate our theory using several numerical examples involving convergence, parametric, and stability analyses for first- and second-order DDE systems. We also include an application of the proposed method to control system design. Conclusions are provided in Section 4.

2. Mathematical Modelling

Consider the following system of n first-order DDEs:

$$\dot{z}_i = f_i(\mathbf{p}, \mathbf{q}_i, t), \quad i = 1, 2, \dots, n, \quad (1)$$

where $\mathbf{p} = [z_1, z_2, \dots, z_n]$ and $\mathbf{q}_i = [z_1(t - \alpha_{i1}), z_2(t - \alpha_{i2}), \dots, z_n(t - \alpha_{in})]$. The delays are $\boldsymbol{\alpha}_i = [\alpha_{i1} > 0, \alpha_{i2} > 0, \dots, \alpha_{in} > 0]$, $i = 1, 2, \dots, n$ and the initial functions are $z_i(t) = \psi_i(t)$, $-\alpha_{im} \leq t \leq 0$, $i = 1, 2, \dots, n$; α_{im} is the maximum delay appearing in $z_i(t)$. Since the delay argument does not appear in the highest-derivative term, (1) is referred to as a retarded DDE. We introduce the following standard transformation [9, 10]:

$$y_i(s, t) \triangleq z_i(t + s), \quad (2)$$

and convert the DDE system (1) and its history functions into the following equivalent initial-boundary value problem:

$$\frac{\partial y_i}{\partial t} = \frac{\partial y_i}{\partial s}, \quad t \geq 0, \quad -\alpha_{im} \leq s \leq 0 \quad (3a)$$

$$\left. \frac{\partial y_i(s, t)}{\partial t} \right|_{s=0} = f_i(\mathbf{u}, \mathbf{v}_i, t) \quad (3b)$$

$$y_i(s, 0) = \psi_i(s), \quad (3c)$$

where

$$\mathbf{u} = [y_1(0, t), y_2(0, t), \dots, y_n(0, t)] \quad (4a)$$

$$\mathbf{v}_i = [y_1(-\alpha_{i1}, t), y_2(-\alpha_{i2}, t), \dots, y_n(-\alpha_{in}, t)]. \quad (4b)$$

Here, $y_i(0, t)$ represents the solution to the DDE (1) when $s = 0$. Several methods have been proposed in the literature to incorporate the boundary condition (3b) when discretizing the PDE (3a), such as the tau and Lagrange multiplier methods.

2.1. Embedded boundary method

We now present our procedure for embedding the boundary condition into the PDE, thereby eliminating the boundary condition from the formulation. We first rewrite (3b) exploiting the equivalence of partial derivatives in space and time (3a):

$$\left. \frac{\partial y_i(s, t)}{\partial s} \right|_{s=0} - f_i(\mathbf{u}, \mathbf{v}_i, t) = 0. \quad (5)$$

Next, we combine the PDE (3a) and the boundary condition (3b):

$$\frac{\partial y_i}{\partial t} = \frac{\partial y_i}{\partial s} + \left(\left. \frac{\partial y_i(s, t)}{\partial t} \right|_{s=0} - f_i(\mathbf{u}, \mathbf{v}_i, t) \right) \delta(s), \quad (6)$$

where $\delta(s)$ is the Dirac delta function. We can see that collocating the PDE at any point on the domain $-\alpha_{im} \leq s < 0$ satisfies (3a), and by collocating at the boundary $s = 0$, we recover the boundary condition (5). We now assume an N -term series solution $y_i(s, t)$ for the PDE:

$$y_i(s, t) = \boldsymbol{\phi}_i(s)^T \boldsymbol{\eta}_i(t), \quad (7)$$

where $\boldsymbol{\phi}_i(s) = [\phi_1(s), \phi_2(s), \dots, \phi_N(s)]^T$ are the global shape functions and $\boldsymbol{\eta}_i(t) = [\eta_{i1}(t), \eta_{i2}(t), \dots, \eta_{iN}(t)]^T$ are the independent coordinates. Shifted Legendre polynomials are used as global shape functions:

$$\phi_1(s) = 1 \quad (8a)$$

$$\phi_2(s) = 1 + \frac{2s}{\tau} \quad (8b)$$

$$\phi_i(s) = \frac{(2i-3)\phi_2(s)\phi_{i-1}(s) - (i-2)\phi_{i-2}(s)}{i-1}, \quad i = 3, 4, \dots, N. \quad (8c)$$

In retarded DDEs, where the order of the delayed arguments is less than that of the highest-order derivative, the solution will become smoother with every knot [17]. If the solution is C^0 -continuous at time $t = 0$, for example, the solution will be C^1 -continuous after time $t = \tau$ (the first knot) and C^n -continuous after n knots. Retarded DDEs always eventually become smooth, which is the reason this approximation is effective.

Upon substituting the series solution (7) into (6), we obtain the following:

$$\boldsymbol{\phi}_i(s)^T \dot{\boldsymbol{\eta}}_i(t) = \boldsymbol{\phi}'_i(s)^T \boldsymbol{\eta}_i(t) + (\boldsymbol{\phi}_i(0)^T \dot{\boldsymbol{\eta}}_i(t) - f_i(\mathbf{u}, \mathbf{v}_i, t)) \delta(s), \quad i = 1, 2, \dots, n, \quad (9)$$

where $\phi_i'(s) \equiv \partial\phi_i(s)/\partial s$. Finally, we pre-multiply both sides of (9) by $\phi_i(s)$, integrate over the domain $s \in [-\alpha_{im}, 0]$, and collect the terms involving $\dot{\boldsymbol{\eta}}_i(t)$ to obtain a system of ODEs:

$$\mathbf{M}_i \dot{\boldsymbol{\eta}}_i(t) = \mathbf{K}_i \boldsymbol{\eta}_i(t) - \phi_i(0) f_i(\mathbf{u}, \mathbf{v}_i, t), \quad i = 1, 2, \dots, n, \quad (10)$$

where

$$\mathbf{M}_i = \int_{-\alpha_{im}}^0 \phi_i(s) \phi_i(s)^T ds - \phi_i(0) \phi_i(0)^T \triangleq \mathbf{A}_i - \phi_i(0) \phi_i(0)^T \quad (11a)$$

$$\mathbf{K}_i = \int_{-\alpha_{im}}^0 \phi_i(s) \phi_i'(s)^T ds. \quad (11b)$$

Note that we can represent the solution using any complete set of basis functions (e.g., Chebyshev, Lagrange, and Hermite polynomials). In this work, we use shifted Legendre polynomials as global shape functions since they allow us to write the entries of matrices \mathbf{A}_i and \mathbf{K}_i in closed form as follows:

$$\mathbf{A}_{cd} = \frac{\alpha_{im}}{2c-1} \delta_{cd} \quad c = 1, 2, \dots, N; d = 1, 2, \dots, N \quad (12a)$$

$$\mathbf{K}_{cd} = \begin{cases} 2, & \text{if } c < d \text{ and } c + d \text{ is odd} \\ 0, & \text{otherwise} \end{cases} \quad c = 1, 2, \dots, N; d = 1, 2, \dots, N. \quad (12b)$$

We now determine the initial conditions for the ODE system. In (10), the term $f_i(\mathbf{u}, \mathbf{v}_i, t)$ can be obtained by substituting the series solution (7) into the expressions for \mathbf{u} and \mathbf{v}_i (4):

$$\mathbf{u} = [\phi_1(0)^T \boldsymbol{\eta}_1(t), \phi_2(0)^T \boldsymbol{\eta}_2(t), \dots, \phi_n(0)^T \boldsymbol{\eta}_n(t)] \quad (13a)$$

$$\mathbf{v}_i = [\phi_1(-\alpha_{i1})^T \boldsymbol{\eta}_1(t), \phi_2(-\alpha_{i2})^T \boldsymbol{\eta}_2(t), \dots, \phi_n(-\alpha_{in})^T \boldsymbol{\eta}_n(t)]. \quad (13b)$$

We now substitute the series solution (7) into the initial conditions (3c):

$$\psi_i(s) = \phi_i^T(s) \boldsymbol{\eta}_i(0), \quad i = 1, 2, \dots, n. \quad (14)$$

Finally, we pre-multiply both sides of (14) by $\phi_i(s)$ and integrate over the domain $s \in [-\alpha_{im}, 0]$ to obtain the following initial conditions for the ODE system:

$$\boldsymbol{\eta}_i(0) = \mathbf{A}_i^{-1} \int_{-\alpha_{im}}^0 \phi_i(s) \psi_i(s) ds, \quad i = 1, 2, \dots, n, \quad (15)$$

where \mathbf{A}_i is defined in (11a). Thus, we have converted the original DDE (1) into a system of ODEs (10) with initial conditions given by (15). The ODEs can be solved numerically to obtain $\boldsymbol{\eta}_i(t)$, whereupon an approximate solution for the DDE (1) can be obtained as follows:

$$y_i(0, t) = \eta_{i0}(t) = \phi_i(0)^T \boldsymbol{\eta}_i(t). \quad (16)$$

We define the following error metric to quantify how well the solutions of (6)

satisfy the original boundary conditions (3b):

$$e_i(t) = \left. \frac{\partial y_i}{\partial t} \right|_{0,t} - f_i = \phi_i(0)^T \dot{\boldsymbol{\eta}}_i(t) - f_i, \quad i = 1, 2, \dots, n. \quad (17)$$

In the sequel, we use a 2-norm to establish the error associated with all boundary conditions:

$$e(t) = \sqrt{e_1(t)^2 + e_2(t)^2 + \dots + e_n(t)^2}. \quad (18)$$

We now compare the proposed formulation to the tau and Lagrange multiplier methods, the two most common strategies for obtaining approximate solutions to DDEs.

2.2. Tau method

In the tau method, the series solution (7) is first substituted into the equivalent system of PDEs (3a):

$$\phi_i(s)^T \dot{\boldsymbol{\eta}}_i(t) = \phi_i'(s)^T \boldsymbol{\eta}_i(t), \quad i = 1, 2, \dots, n. \quad (19)$$

Pre-multiplying both sides of (19) by $\phi_i(s)$ and integrating over the domain $s \in [-\alpha_{im}, 0]$, we obtain the following system of ODEs:

$$\mathbf{A}_i \dot{\boldsymbol{\eta}}_i(t) = \mathbf{K}_i \boldsymbol{\eta}_i(t), \quad i = 1, 2, \dots, n, \quad (20)$$

where \mathbf{A}_i and \mathbf{K}_i are defined in (11a) and (11b), respectively. Next, we substitute the series solution (7) into the boundary condition (3b):

$$\phi_i(s)^T \dot{\boldsymbol{\eta}}_i(t) = f_i(\mathbf{u}, \mathbf{v}_i, t), \quad i = 1, 2, \dots, n, \quad (21)$$

where \mathbf{u} and \mathbf{v}_i are defined in (4). The boundary condition (21) is then incorporated into the ODEs (20) by replacing the last row of \mathbf{A}_i and \mathbf{K}_i in (20) with the boundary condition. Thus, we arrive at the following system of ODEs:

$$\mathbf{A}_{iTau} \dot{\boldsymbol{\eta}}_i(t) = \mathbf{K}_{iTau} \boldsymbol{\eta}_i(t) + \mathbf{F}_{iTau}, \quad i = 1, 2, \dots, n, \quad (22)$$

where \mathbf{A}_{iTau} , \mathbf{K}_{iTau} , and \mathbf{F}_{iTau} are defined as follows:

$$\mathbf{A}_{iTau} = \begin{bmatrix} \bar{\mathbf{A}}_i \\ \phi_i(0)^T \end{bmatrix}, \quad \mathbf{K}_{iTau} = \begin{bmatrix} \bar{\mathbf{K}}_i \\ 0 \end{bmatrix}, \quad \mathbf{F}_{iTau} = \left\{ \begin{array}{c} \mathbf{0} \\ f_i(\mathbf{u}, \mathbf{v}_i, t) \end{array} \right\}. \quad (23)$$

Matrices $\bar{\mathbf{A}}_i$ and $\bar{\mathbf{K}}_i$ are obtained by deleting the last row of \mathbf{A}_i and \mathbf{K}_i , respectively. Finally, the system of ODEs (22) is integrated forward in time, using the initial condition given in (15), to obtain an approximate solution for the original DDE system (1):

$$y_i(0, t) = \eta_{i0}(t) = \phi_i(0)^T \boldsymbol{\eta}_i(t). \quad (24)$$

2.3. Lagrange multiplier method

Another widely used method to obtain an approximate solution for a system of DDEs is the Lagrange multiplier method, where the boundary constraint (3b) is enforced by Lagrange multipliers. We first write the PDE (3a) as follows:

$$\frac{\partial y_i}{\partial t} = \frac{\partial y_i}{\partial s} + \delta(s)\gamma_i(t), \quad i = 1, 2, \dots, n, \quad (25)$$

where $\gamma_i(t)$ denotes the (time-dependent) Lagrange multiplier. On substituting the series solution (7) into (25), we obtain the following:

$$\phi_i(s)^T \dot{\boldsymbol{\eta}}_i(t) = \phi_i'(s)^T \boldsymbol{\eta}_i(t) + \delta(s)\gamma_i(t), \quad i = 1, 2, \dots, n. \quad (26)$$

Pre-multiplying both sides of (26) by $\phi_i(s)$ and integrating over the domain $s \in [-\alpha_{im}, 0]$ yields the following:

$$\mathbf{A}_i \dot{\boldsymbol{\eta}}_i(t) = \mathbf{K}_i \boldsymbol{\eta}_i(t) + \phi_i(0)\gamma_i(t), \quad i = 1, 2, \dots, n, \quad (27)$$

where \mathbf{A}_i and \mathbf{K}_i are defined in (11a) and (11b), respectively. We now substitute the series solution (7) into the boundary condition (3b):

$$\phi_i(0)^T \dot{\boldsymbol{\eta}}_i(t) = f_i(\mathbf{u}, \mathbf{v}_i, t), \quad i = 1, 2, \dots, n, \quad (28)$$

where \mathbf{u} and \mathbf{v}_i are defined in (4). We now use (27) and (28) to obtain the following expression for the Lagrange multiplier $\gamma_i(t)$:

$$\gamma_i(t) = \frac{f_i(\mathbf{u}, \mathbf{v}_i, t) - \phi_i(0)^T \mathbf{A}_i^{-1} \mathbf{K}_i \boldsymbol{\eta}_i(t)}{\phi_i(0)^T \mathbf{A}_i^{-1} \phi_i(0)}, \quad i = 1, 2, \dots, n. \quad (29)$$

Finally, we substitute (29) into (27) and, using the initial condition given in (15), integrate the ODEs forward in time to obtain $\boldsymbol{\eta}_i(t)$; the approximate solution is then given by the following:

$$y_i(0, t) = \eta_{i0}(t) = \phi_i(0)^T \boldsymbol{\eta}_i(t). \quad (30)$$

In summary, we have developed a method to convert a system of DDEs into a system of PDEs without any boundary conditions. The PDEs are discretized using the Galerkin method and converted into a system of ODEs, which can then be solved numerically. As will be demonstrated in Section 3, our approach satisfies the original boundary conditions with only small amounts of error, and produces results that compare favourably with those obtained using the tau and Lagrange multiplier methods.

3. Numerical Studies

In this section, we present four test cases to investigate the accuracy of the approximation method we propose. The developed theory is applied to systems of first- and second-order DDEs. The numerical results for the proposed method are obtained using the `ode15s` solver in Matlab, and are compared to those obtained

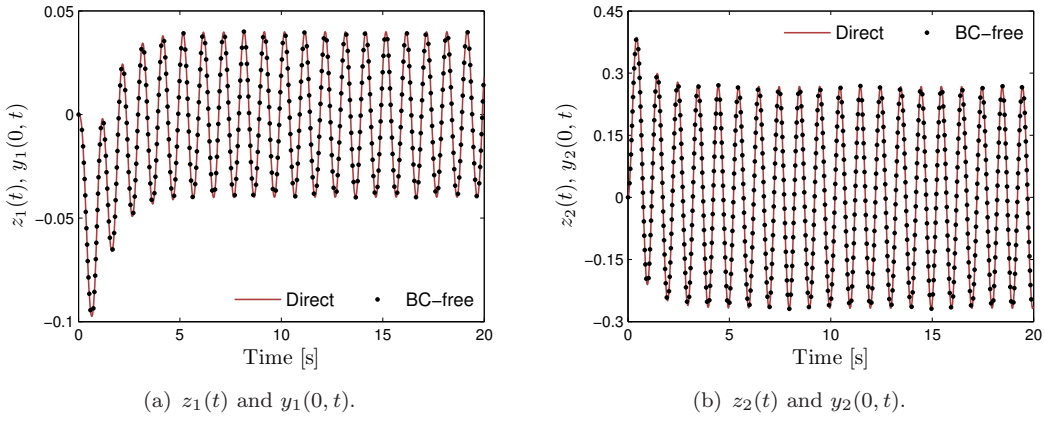


Figure 1. Comparison of direct numerical solution $z_i(t)$ and solution obtained using the Galerkin method $y_i(0, t)$ for (31). The parameters are $b_1 = b_6 = 2$, $b_2 = b_4 = \alpha_{22} = 1$, $b_3 = b_7 = b_8 = \alpha_{11} = 0.1$, $b_5 = 0.75$, $\alpha_{12} = 0.3$, $\alpha_{21} = 0.5$, $F = 1.8$, $\omega = 2\pi$, and $N = 7$.

by integrating the DDEs directly using the `dde23` [18] solver. Relative and absolute integration tolerances of 10^{-8} are used throughout.

3.1. Coupled first-order DDEs

Consider the following system of retarded DDEs:

$$\dot{z}_1(t) + b_1 z_1(t) + b_2 z_2(t) + b_3 z_1(t - \alpha_{11}) + b_4 z_2(t - \alpha_{12})^3 = 0 \quad (31a)$$

$$\dot{z}_2(t) + b_5 z_1(t) + b_6 z_2(t) + b_7 z_1(t - \alpha_{21}) + b_8 z_2(t - \alpha_{22})^3 = F \sin(\omega t). \quad (31b)$$

This is a nonlinear system of coupled DDEs containing delays in both z_1 and z_2 . The initial history functions are assumed to be the following:

$$z_1(t) = 0, \quad -\max(\alpha_{11}, \alpha_{21}) \leq t \leq 0 \quad (32a)$$

$$z_2(t) = 0, \quad -\max(\alpha_{12}, \alpha_{22}) \leq t \leq 0. \quad (32b)$$

In Figure 1, we compare the displacements $y_1(0, t)$ and $y_2(0, t)$ obtained using the Galerkin method to those obtained using the `dde23` solver in Matlab; the parameters are provided in the figure caption. Clearly, the results obtained using the Galerkin method match the direct numerical integration of (31). In Figure 2, we plot the least-square errors for $y_1(0, t)$ and $y_2(0, t)$ as functions of the number of terms N used in the series approximation (7):

$$E_{LS} = \sum_{k=1}^{10000} (z(t_k) - y_1(0, t_k))^2. \quad (33)$$

The simulation was performed for $t \in [0, 20]$, which was divided into 10,000 equidistant points to compute the error (33). As shown in Figure 2, $N = 7$ terms are sufficient to achieve an error of 0.01. Also note that the error associated with all methods decreases as N increases, indicating convergence.

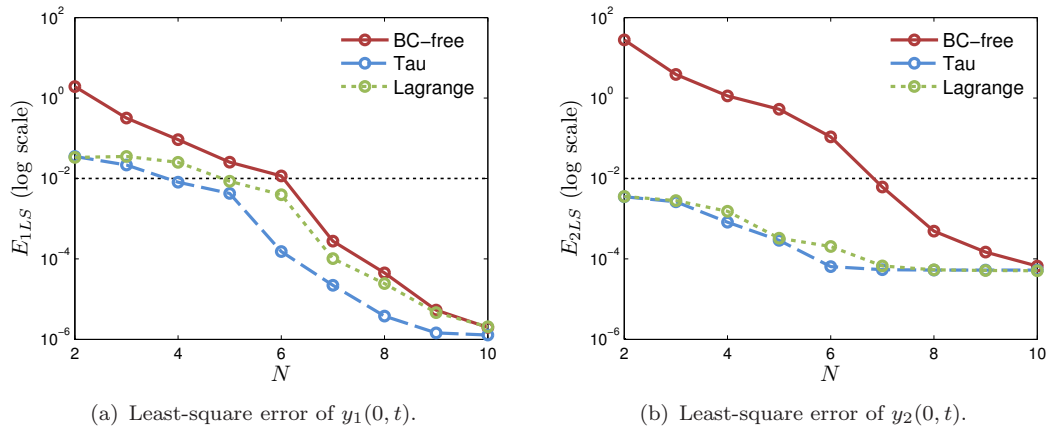


Figure 2. Results of convergence studies indicate that $N = 7$ terms are sufficient to obtain converged solutions. We define convergence as having least-square error less than 0.01 (horizontal line).

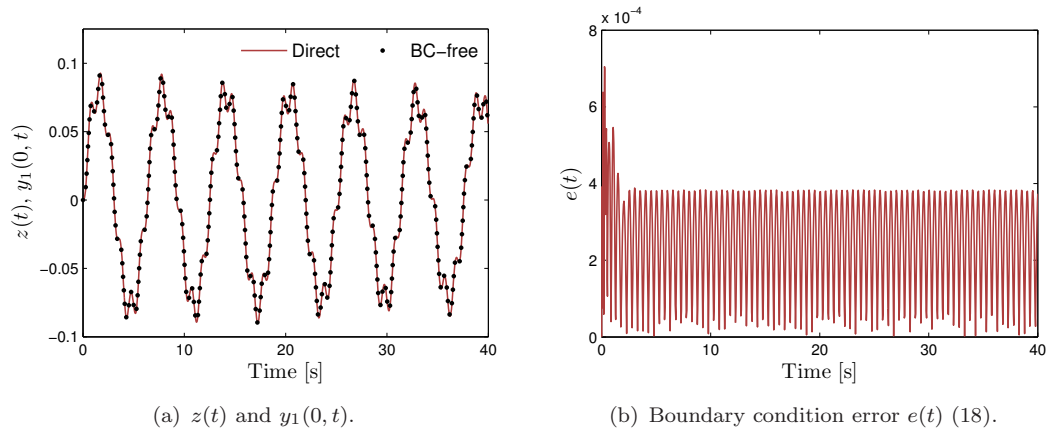


Figure 3. Comparison of direct numerical solution $z(t)$ and solution obtained using the Galerkin method $y_1(0, t)$ for (34). The parameters are $b_1 = 0.01$, $b_2 = b_3 = \alpha = 1$, $b_4 = 0$, $\beta = F = 0.5$, $\omega = 2\pi$, and $N = 7$.

3.2. Second-order DDE

To test the developed formulation for higher-order DDEs, we now consider the following second-order nonlinear DDE:

$$\ddot{z}(t) + b_1 \dot{z}(t) + b_2 z(t) + b_3 z(t - \alpha)^3 + b_4 \dot{z}(t - \beta) = F \sin(\omega t), \quad (34)$$

which contains delays in both $z(t)$ and $\dot{z}(t)$. The initial history functions are assumed to be $z(t) = \dot{z}(t) = 0$, $-1 \leq t \leq 0$. In Figures 3, 4, and 5, we compare the displacement $y_1(0, t)$ obtained using the Galerkin method to that obtained using the `dde23` solver in Matlab using three sets of parameters (provided in the figure captions). In all three cases, the results obtained using the Galerkin method are in good agreement with the direct numerical integration of (34). In Figure 3(b), we show that the error associated with satisfying the boundary conditions is less than 8×10^{-4} using the first set of parameters; the absolute error is also low, as shown in Figure 4(b) for the second parameter set. In Figure 5(b), we plot the least-square error as a function of the number of terms N used in the series approximation (7). The simulation was performed for $t \in [0, 100]$, which was divided into 10,000 equidistant points to compute the error (33). As shown in Figure 5(b), con-

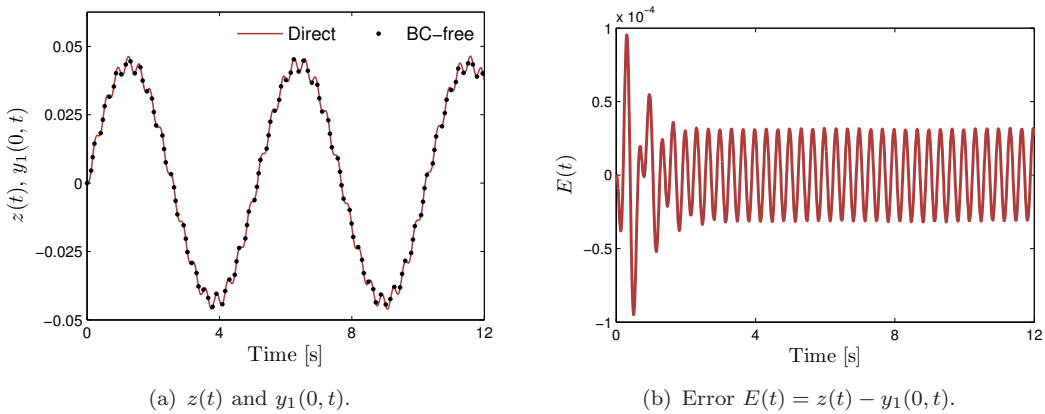


Figure 4. Comparison of direct numerical solution $z(t)$ and solution obtained using the Galerkin method $y_1(0,t)$ for (34). The parameters are $b_1 = b_4 = 0$, $b_2 = 1.5$, $b_3 = 0.1$, $\alpha = F = 1$, $\beta = 0.5$, $\omega = 6\pi$, and $N = 7$.

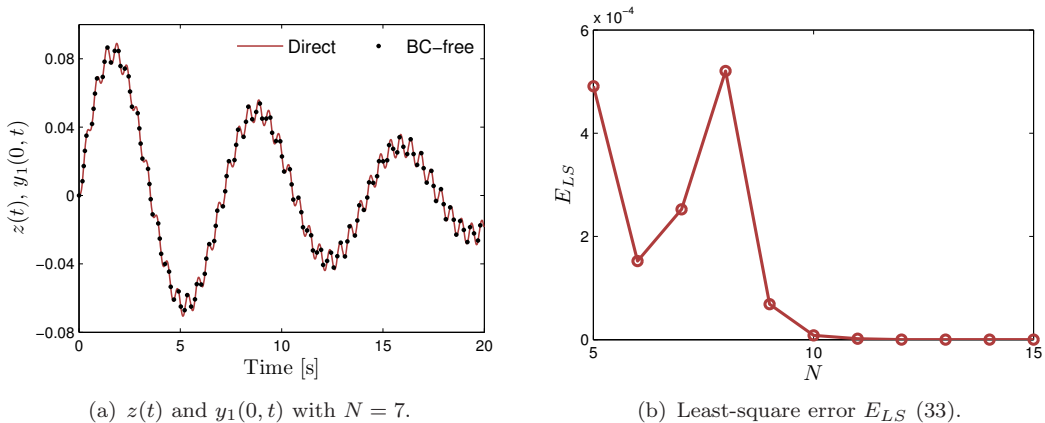


Figure 5. Comparison of direct numerical solution $z(t)$ and solution obtained using the Galerkin method $y_1(0,t)$ for (34) when the velocity delay term is nonzero. The parameters are $b_1 = 0.05$, $b_2 = 0.75$, $b_3 = \alpha = F = 1$, $b_4 = 0.1$, $\beta = 0.5$, and $\omega = 4\pi$.

vergence is achieved at $N = 11$, and the least-square error remains below 6×10^{-4} even when only 5 terms are retained in the series solution.

3.3. Stability charts

For linear DDEs, (10) takes the following form:

$$\dot{\eta} = C\eta, \tag{35}$$

where $\eta = [\eta_1(t), \eta_2(t), \dots, \eta_n(t)]^T$. The stability of linear DDEs can be analyzed by evaluating the stability of the ODEs obtained from the Galerkin approximation (35). The characteristic equation for a DDE is a quasi-polynomial with an infinite number of roots; to ascertain stability, we must determine whether all the roots have negative real parts. The roots of the characteristic equation can be found using a nonlinear solver; however, providing the solver with good initial guesses is a nontrivial task. In contrast, the Galerkin approximation of a linear DDE results in a system of ODEs of the form shown in (35), and we can directly evaluate the

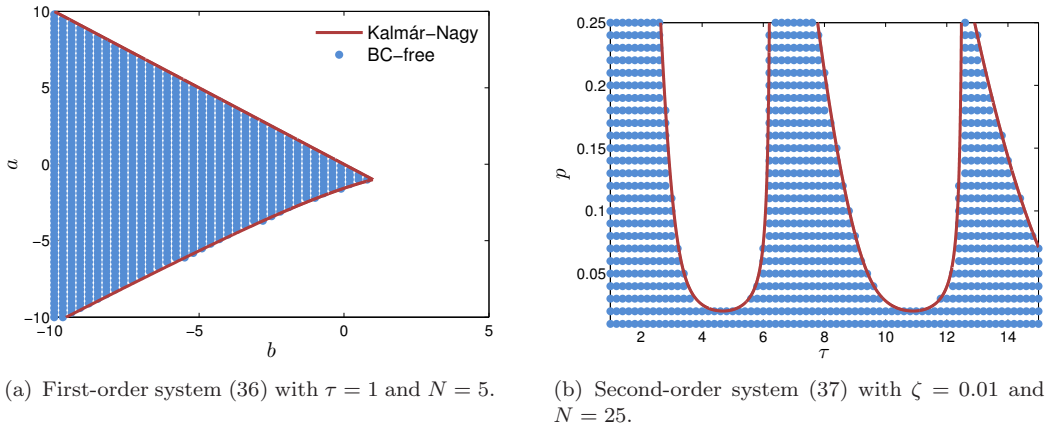


Figure 6. Stability regions obtained analytically (red lines) and using the Galerkin method (blue dots) for first- and second-order systems.

eigenvalues of these ODEs to establish system stability. In fact, the eigenvalues of (35) approximate the characteristic roots [19] of the original DDEs, and the approximation becomes increasingly accurate as the number of terms in the series solution is increased. The system is stable if all eigenvalues of (35) have negative real parts.

Consider the following equation:

$$\dot{x}(t) = ax(t) + bx(t - \tau). \tag{36}$$

The stability of (36) changes as we vary parameters a and b . Figure 6(a) shows the stability diagram for (36) with $\tau = 1$. The region within the red lines is the stable region, as reported previously [20]; the blue dots indicate the same stable region, determined using the Galerkin method with $N = 5$. We have also studied the stability of a second-order system that arises in the study of machine tool vibration [21]:

$$\ddot{x}(t) + 2\zeta\dot{x}(t) + (1 + p)x(t) - px(t - \tau) = 0. \tag{37}$$

Figure 6(b) shows the stability diagram for (37) with $\zeta = 0.01$ as p and τ vary. The red lines indicate the stable region determined analytically [21]. Once again, the blue dots indicate that the same stable region is obtained using the Galerkin method.

3.4. Application to control

Numerical integration of a DDE using the `dde23` solver will generally be faster than integrating a set of ODEs obtained using the Galerkin approximation. The real advantage of the proposed formulation lies in the design of observers, filters, and control systems for physical processes governed by DDEs. Modern control theory often assumes that the plant model can be approximated using ODEs, and several theoretical proofs are available for such models. Control theory for DDEs, on the other hand, is a topic of ongoing research [22], and the authors believe the field is underdeveloped. In this example, we apply the proposed boundary condition-free formulation to a control problem to take advantage of control theory developed for systems described by ODEs.

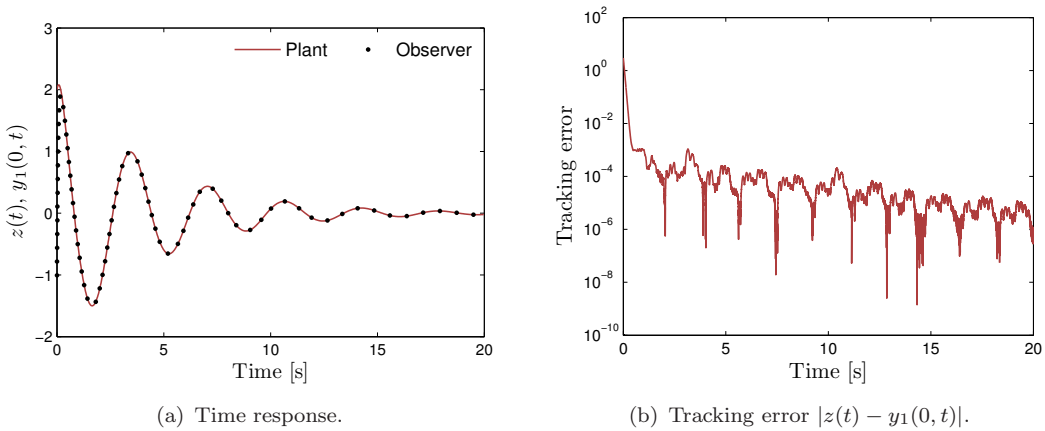


Figure 7. Comparison of plant output $z(t)$ and observer output $y_1(0, t)$ for (38). $N = 20$ terms were used in the Galerkin approximation.

Consider a process governed by the following second-order DDE:

$$\ddot{z} + 2\zeta\dot{z} + k_1z + k_2z(t - \tau) = 0, \quad (38)$$

where the parameters are $\zeta = 2$, $k_1 = k_2 = 5$, and $\tau = 1$. The objective is to design an observer that can accurately track the response of the DDE (38). We obtain the plant output by integrating the DDE numerically using the following history functions:

$$\dot{z}(t) = z(t) = 2, \quad t \in [-1, 0]. \quad (39)$$

We then use the approximate ODEs with history functions $\dot{z}(t) = z(t) = -1, t \in [-1, 0]$ to track the plant response, whereupon traditional control strategies can be applied. Since (38) is a second-order DDE, retaining N terms in the series solution results in a system of first-order ODEs of size $2N$ (corresponding to N displacements and N velocities). Inspired by the theory of high-gain observers [23], we add $20(z(t) - y_1(0, t))$ to the first displacement-level ODE and $20(\dot{z}(t) - y_2(0, t))$ to the first velocity-level ODE. Here, $y_1(0, t)$ and $y_2(0, t)$ indicate the observer output for displacement and velocity, respectively. Finally, we integrate the ODEs forward in time and compare the plant and observer outputs. As shown in Figure 7, the observer output $y_1(0, t)$ is in very good agreement with the plant output $z(t)$, and the tracking error quickly becomes negligible. This example clearly demonstrates that the proposed method can be used for control purposes (such as designing observers, filters, and controllers) for systems governed by retarded DDEs.

4. Conclusions

We have, for the first time, transformed a given DDE into an equivalent PDE without any boundary conditions. This formulation allows us to apply the Galerkin method to the PDE without taking any special care to incorporate boundary conditions (using Lagrange multipliers or the tau method, for example). Legendre polynomials are used as the basis functions in the Galerkin method, and we ultimately obtain finite-dimensional ODE approximations of the original DDEs. We have demonstrated with several numerical examples that the ODEs obtained us-

ing our PDE formulation accurately capture the dynamics of the original DDEs. Convergence is attained by increasing the number of terms in the Galerkin approximation. This formulation allows us to exploit existing tools developed for ODE systems to analyze DDEs.

Acknowledgements

The authors thank the anonymous referees for their many helpful suggestions. C.P.V. gratefully acknowledges the Department of Science and Technology for funding this research through the Fast Track Scheme for Young Scientists (Ref:SB/FTP/ETA-0462/2012).

References

- [1] R.D. Driver, *Ordinary and Delay Differential Equations*, Applied Mathematical Sciences, Vol. 20, Springer, New York, 1977.
- [2] J.P. Richard, *Time-delay systems: an overview of some recent advances and open problems*, *Automatica* 39 (2003), pp. 1667–1694.
- [3] G.A. Bocharov and F.A. Rihan, *Numerical modelling in biosciences using delay differential equations*, *Journal of Computational and Applied Mathematics* 125 (2000), pp. 183–199.
- [4] T. Insperger and G. Stépán, *Stability of the milling process*, *Periodica Polytechnica* 44 (2000), pp. 47–57.
- [5] B. Balachandran, *Nonlinear dynamics of milling processes*, *Philosophical Transactions of the Royal Society A: Mathematical, Physical and Engineering Sciences* 359 (2001), pp. 793–819.
- [6] M.P. Paidoussis, *Fluid-Structure Interactions: Slender Structures and Axial Flow*, Vol. 1, Academic Press, San Diego, 1998.
- [7] L.A. Safonov, E. Tomer, V.V. Strygin, Y. Ashkenazy, and S. Havlin, *Multifractal chaotic attractors in a system of delay-differential equations modeling road traffic*, *Chaos: An Interdisciplinary Journal of Nonlinear Science* 12 (2002), pp. 1006–1014.
- [8] P. Wahi and A. Chatterjee, *Galerkin projections for delay differential equations*, *ASME Journal of Dynamic Systems, Measurement, and Control* 127 (2005), pp. 80–87.
- [9] T. Koto, *Method of lines approximations of delay differential equations*, *Computers and Mathematics with Applications* 48 (2004), pp. 45–59.
- [10] S. Maset, *Numerical solution of retarded functional differential equations as abstract Cauchy problems*, *Journal of Computational and Applied Mathematics* 161 (2003), pp. 259–282.
- [11] A.H. Nayfeh and D.T. Mook, *Nonlinear Oscillations*, Wiley, New York, 1979.
- [12] W.F.J. Govaerts, *Numerical Methods for Bifurcations of Dynamical Equilibria*, Society for Industrial and Applied Mathematics, Philadelphia, 2000.
- [13] A. Dhooge, W. Govaerts, Y.A. Kuznetsov, H.G.E. Meijer, and B. Sautois, *New features of the software MatCont for bifurcation analysis of dynamical systems*, *Mathematical and Computer Modelling of Dynamical Systems* 14 (2008), pp. 147–175.
- [14] C.P. Vyasarayani, *Galerkin approximations for higher order delay differential equations*, *ASME Journal of Computational and Nonlinear Dynamics* 7 (2012), p. 031004.
- [15] K. Ito and R. Teglas, *Legendre-tau approximations for functional-differential equations*, *SIAM Journal on Control and Optimization* 24 (1986), pp. 737–759.
- [16] A. de Jesus Kozakevicius and T. Kalmár-Nagy, *Weak formulation for delay equations*, in *Proceedings of the 9th Brazilian Conference on Dynamics, Control and their Applications*, Serra Negra, Brazil, 2010, pp. 732–736.
- [17] M. Roussel, *Chemistry 5850: Nonlinear Dynamics, Lecture 11: Delay-*

- differential equations*, Lecture notes, University of Lethbridge (2004), <http://people.uleth.ca/~rousseau/nld/delay.pdf>.
- [18] L.F. Shampine and S. Thompson, *Solving delay differential equations with dde23*, Southern Methodist University and Radford University (2000), <http://www.radford.edu/~thompson/webddes/tutorial.pdf>.
- [19] C.P. Vyasarayani, S. Subhash, and T. Kalmár-Nagy, *Spectral approximations for characteristic roots of delay differential equations*, International Journal of Dynamics and Control 2 (2014), pp. 126–132.
- [20] T. Kalmár-Nagy, *Stability analysis of delay-differential equations by the method of steps and inverse Laplace transform*, Differential Equations and Dynamical Systems 17 (2009), pp. 185–200.
- [21] T. Kalmár-Nagy, G. Stépán, and F.C. Moon, *Subcritical Hopf bifurcation in the delay equation model for machine tool vibrations*, Nonlinear Dynamics 26 (2001), pp. 121–142.
- [22] J.P. Richard, *Time-delay systems: an overview of some recent advances and open problems*, Automatica 39 (2003), pp. 1667–1694.
- [23] H.K. Khalil and J.W. Grizzle, *Nonlinear Systems*, Prentice Hall, Englewood Cliffs, 2002.

Figure Captions

Figure 1: Comparison of direct numerical solution $z_i(t)$ and solution obtained using the Galerkin method $y_i(0, t)$ for (31). The parameters are $b_1 = b_6 = 2$, $b_2 = b_4 = \alpha_{22} = 1$, $b_3 = b_7 = b_8 = \alpha_{11} = 0.1$, $b_5 = 0.75$, $\alpha_{12} = 0.3$, $\alpha_{21} = 0.5$, $F = 1.8$, $\omega = 2\pi$, and $N = 7$.

Figure 2: Results of convergence studies indicate that $N = 7$ terms are sufficient to obtain converged solutions. We define convergence as having least-square error less than 0.01 (horizontal line).

Figure 3: Comparison of direct numerical solution $z(t)$ and solution obtained using the Galerkin method $y_1(0, t)$ for (34). The parameters are $b_1 = 0.01$, $b_2 = b_3 = \alpha = 1$, $b_4 = 0$, $\beta = F = 0.5$, $\omega = 2\pi$, and $N = 7$.

Figure 4: Comparison of direct numerical solution $z(t)$ and solution obtained using the Galerkin method $y_1(0, t)$ for (34). The parameters are $b_1 = b_4 = 0$, $b_2 = 1.5$, $b_3 = 0.1$, $\alpha = F = 1$, $\beta = 0.5$, $\omega = 6\pi$, and $N = 7$.

Figure 5: Comparison of direct numerical solution $z(t)$ and solution obtained using the Galerkin method $y_1(0, t)$ for (34) when the velocity delay term is nonzero. The parameters are $b_1 = 0.05$, $b_2 = 0.75$, $b_3 = \alpha = F = 1$, $b_4 = 0.1$, $\beta = 0.5$, and $\omega = 4\pi$.

Figure 6: Stability regions obtained analytically (red lines) and using the Galerkin method (blue dots) for first- and second-order systems.

Figure 7: Comparison of plant output $z(t)$ and observer output $y_1(0, t)$ for (38). $N = 20$ terms were used in the Galerkin approximation.